[Article ID] 1003- 6326(2001)05- 0691- 05

Ternary alloying of Mo_5Si_3 with Zr, Ti, Co and V①

CAO Yu(曹 昱), YI Dan-qing(易丹青), LU Bin(卢 斌),
DU Ruo-xin(杜若昕), SHU Jin-bo(舒金波)
(Department of Materials Science and Engineering, Central South University,
Changsha 410083, P. R. China)

[Abstract] The Mo_5Si_3 base alloys with a series of transition metal elements were prepared by arc-melting, and were annealed at 1250 ℃ in vacuum for 24 h. Ternary alloying effect was investigated by X-ray diffractometry (XRD), optical microscopy, scanning electron microscopy (SEM) and energy dispersive spectroscopy(EDS). The EDS results show that Zr, Ti, Co and V have certain solubility in homogenized Mo_5Si_3, which are determined to be 2.20±1.42, 15.94±0.18, 3.33±0.76 and 7.43±0.22 (mole fraction, %), respectively. Microstructural characteristics indicate that all studied alloys have a two-phase microstructure, i. e., Mo_5Si_3 matrix and the second phase $Mo_{37}Zr_{20}Si_{43}$, $Mo_{66}Si_{19}Ti_{15}$, MoCoSi or $(Mo, V)_3Si$.

[Key words] silicides; alloying effect; microstructure
[CLC number] TG 146.4 [Document code] A

1 INTRODUCTION

Silicides are used as various protective coatings against wear, corrosion and oxidation, and as integrated circuit films because of their high hardness, high electrical and thermal conductivity and good oxidation resistance at high temperatures. In particular, $MoSi_2$ is put into industrial production as heating elements in high-temperature furnaces[1,2]. Meanwhile, refractory silicides are promising candidate materials for high temperature structural applications because of their high melting point, high elastic module and good resistance against oxidation and corrosion etc. Now, it is realized that silicides have great potential for replacing carbon/carbon composite and ceramic matrix composite under oxidation conditions at temperatures from 1200 ℃ to 1600 ℃[3].

Mo_5Si_3 is an intermetallic compound of great importance in engineering. It crystallizes in a tetragonal $D8_m$ structure[4]. Its density is 8.24 g/cm^3. The Vickers hardness is 12~ 13 GPa[5]. The electric conductivity coefficient is 218 $\Omega\cdot cm^{-2}$[6]. Compared with $MoSi_2$, the melting point of Mo_5Si_3 is higher and the high temperature creep resistance of $MoSi_2$-Mo_5Si_3 eutectic alloy is better than single phase $MoSi_2$. So Mo_5Si_3 has received special attention in high-temperature structural applications as a matrix or a reinforcing phase. But the poor room temperature ductility and fracture toughness limit its structural utility.

Mo_5Si_3 has the alloying potential and the mechanical properties of Mo_5Si_3 might be improved by adding a series of alloying elements[6]. Firstly, alloying may lead to crystal structure modification, i. e., change from a low-symmetry structure to a high-symmetry structure. Secondly, alloying can change the feature of atomic bonding. Thirdly, alloying may result in the precipitation of second phases[7]. All these sometimes contribute to the increase in ductility and toughness. A well-known example is that the ductility of Ni_3Al was dramatically increased by the microalloying of boron[8]. It is known that Fe, W and Nb exhibit certain solid solubility in Mo_5Si_3[9] and Fe results in crystal structure modification[10]. Likely because of a large complex unite cell, semi-covalent bonding and high barrier to dislocation motion, the increased symmetry of hexagonal Mo_5Si_3C does not result in improved toughness or plasticity at room temperature[11].

The purpose of this work is to investigate the solid solubility of transition metal elements in Mo_5Si_3 and explore the possibility of microstructure and properties modification by alloying with some of these metal elements.

2 EXPERIMENTAL

2.1 Preparation of alloys

High-purity metals (> 99%) were used as starting materials. All the alloys were prepared by the arc melting process. For each composition, several remelts were made in order to ensure the homogeneity of alloys. The composition of the studied alloys are listed in Table 1.

① [Foundation item] Project (59881006) supported by the National Natural Science Foundation of China
[Received date] 2001- 03- 09; [Accepted date] 2001- 06- 06

Table 1 Composition of studied alloys

Sample	Alloying element	Composition(mole fraction, %)
1#	–	Mo_5Si_3
2#	Zr	Mo_4ZrSi_3
3#	Ti	Mo_4TiSi_3
4#	Co	Mo_4CoSi_3
5#	V	Mo_4VSi_3

All the specimens used for experiments were homogenized at 1 250 ℃ for 24 h in vacuum and slowly cooled down to room temperature.

2.2 Characteristics of alloys

The instruments used for the microstructural observation and analysis are a POLYVAR-MET color optical microscope and a KYKY-2800 scanning electron microscope.

The general phase survey was carried out with metallographic specimens by using a SIMENS-500 X-ray diffractometer with CuK_α radiation (λ = 1.5406 Å). Back-scattered electron micrography (BEM) and energy dispersive spectroscopy (EDS) were used for the identification of some precipitated phases. The solid solubility of alloying elements was also determined by EDS.

The microhardness was measured with a MICRO-DUROMAT 4000 microhardnes tester under condition of a fixed load (0.5 N) and a fixed contact time (10 s).

3 RESULTS AND DISCUSSION

3.1 Phase analysis

The X-ray diffraction patterns of alloys 1# ~ 5# are shown in Fig. 1.

For alloy 1#, the XRD result shows the co-existence of Mo_5Si_3 and a second phase Mo_3Si, which is further confirmed by EDS analysis. The existence of Mo_3Si is perhaps because of the deviation of the actual composition from the nominal composition.

The XRD pattern of alloy 2# shows the existence of Mo_5Si_3. From back-scattered electron micrographs, a second phase can be observed. Its composition (apparent composition) given by EDS is shown in Table 2. According to the 1250 ℃ isothermal section of Mo-Si-Zr system phase diagram (as shown in Fig. 2)[6], it is close to phase B ($Mo_{0.31}Zr_{0.22}Si_{0.47}$).

For alloy 3#, only one phase, Mo_5Si_3 is detected by XRD. However, a small amount of precipitated phase is found by metallographic observation at grain boundaries. The composition of the second phase, given by EDS, is $Mo_{66}Si_{19}Ti_{15}$ (apparent composition).

Similarly to above alloys, the XRD patterns of

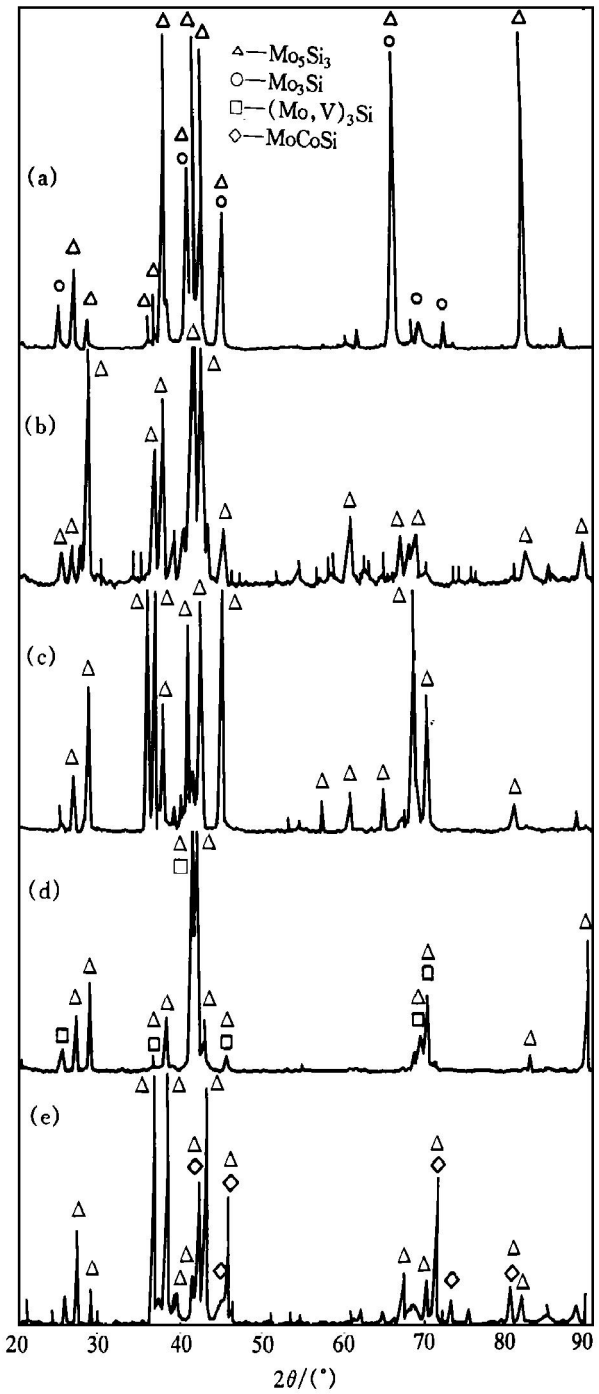

Fig. 1 X-ray diffraction patterns of Mo_5Si_3-based alloys
(a) —Mo_5Si_3; (b) —Mo_4ZrSi_3; (c) —Mo_4TiSi_3; (d) —Mo_4VSi_3; (e) —Mo_4CoSi_3

alloys 4# and 5# show the co-existence of two crystalline phases. Besides the Mo_5Si_3 phase, the second phases identified by XRD and EDS in those two alloys are CoMoSi and $(Mo, V)_3Si$, respectively. Phase analysis results obtained from all five alloys are summarized in Table 2 and Table 3.

3.2 Microstructure of Mo_5Si_3 base alloys

The microstructure of alloy 1# consists of a coarse primary phase Mo_5Si_3 and a dot-like eutectic mixture of Mo_5Si_3 and Mo_3Si, according to XRD and

Table 2 Composition of precipitated phases in ternary Mo_5Si_3 base alloys

Alloy number	Precipitated phase	Chemical composition of alloy phases(mole fraction, %)					
		Zr	Ti	Co	V	Mo	Si
1#	Mo_3Si					77.59±0.16	22.44±0.16
2#	$Mo_{37}Zr_{20}Si_{43}$	20.05±2.91				37.32±2.86	42.63±1.32
3#	$Mo_{66}Ti_{15}Si_{19}$		14.60±3.92			66.08±1.27	19.32±0.99
4#	MoCoSi			37.22±0.04		33.83±0.26	28.95±0.27
5#	$(Mo, V)_3Si$				9.06±0.18	62.26±0.19	28.68±0.13

Table 3 Phases present in homogenized Mo_5Si_3 base alloys

Alloy number	Alloying element and level (mole fraction, %)	Phase
1#	–	Mo_5Si_3, Mo_3Si
2#	12.5Zr	Mo_5Si_3, $Mo_{37}Zr_{20}Si_{43}$
3#	12.5Ti	Mo_5Si_3, $Mo_{66}Si_{19}Ti_{15}$
4#	12.5Co	Mo_5Si_3, MoCoSi
5#	12.5V	Mo_5Si_3, $(Mo, V)_3Si$

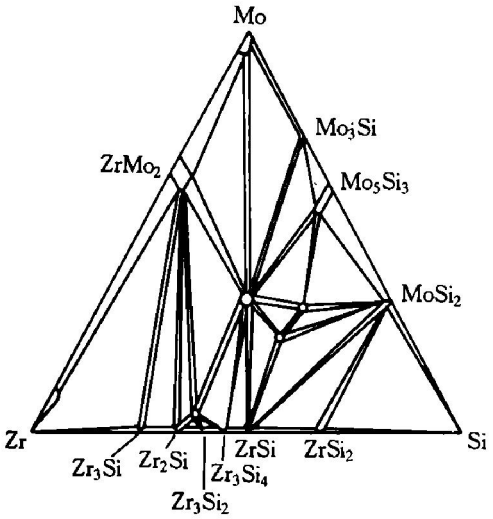

Fig. 2 1250 ℃ isothermal section of Mo-Si-Zr system phase diagram[6]

EDS analysis, as shown in Fig. 3.

In alloy 2#, the second phase, $Mo_{37}Zr_{20}Si_{43}$ has a block-like morphology and discontinuously distributes on the grey Mo_5Si_3 matrix, as shown in Fig. 4.

The microstructure of alloy 3# and 5# is similarly characterized by the matrix phase Mo_5Si_3 and the second phases $Mo_{66}Ti_{15}Si_{19}$ or $(Mo, V)_3Si$, which precipitated on the grain boundary, as shown in Figs. 5 and 6.

Fig. 7 shows micrography of Mo-Si-Co alloy. Mo_5Si_3 and MoCoSi exhibit similar morphology, i.e., long strips parallel to each other. The two phases are somewhat elongated in a certain direction. Microcracks can be easily seen.

3.3 Solubility of transition elements in Mo_5Si_3

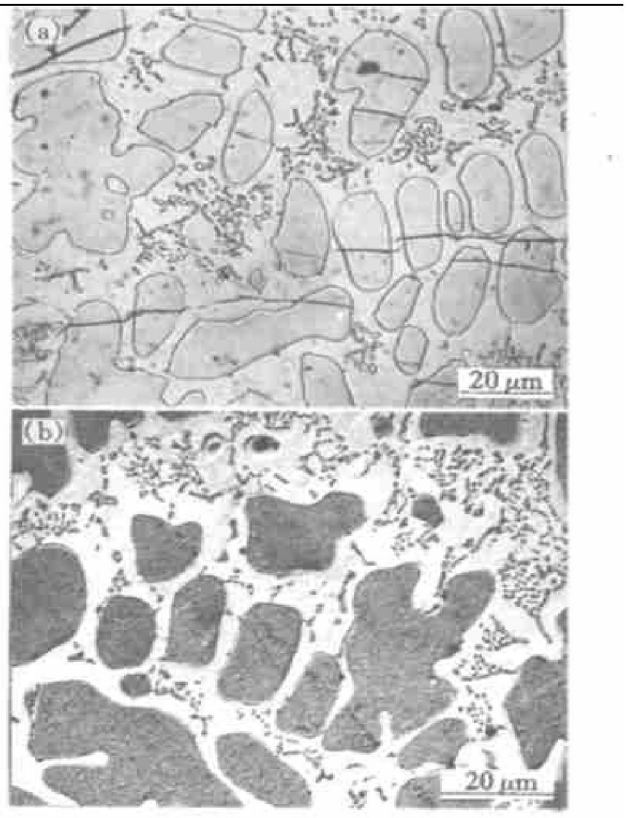

Fig. 3 Microstructure of Mo_5Si_3 alloy
(a) —Optical micrograph;
(b) —Back-scattered electron micrograph

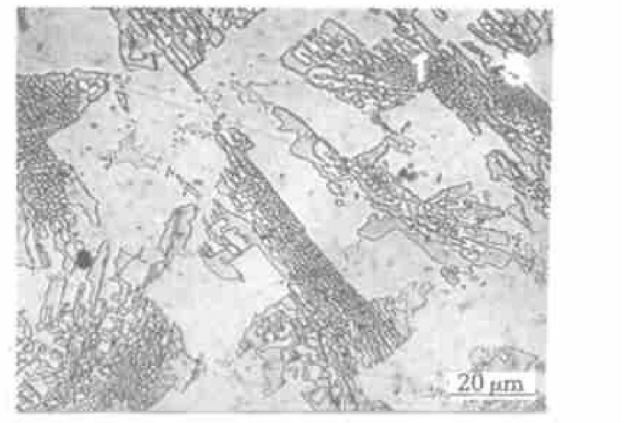

Fig. 4 Microstructure of Mo_4ZrSi_3 alloy

The solubility of alloying elements in Mo_5Si_3, obtained from as-annealed samples in this study, are given in Table 4.

It is found that Zr and Co have limited solubility in homogenized Mo_5Si_3; while Ti and V have larger

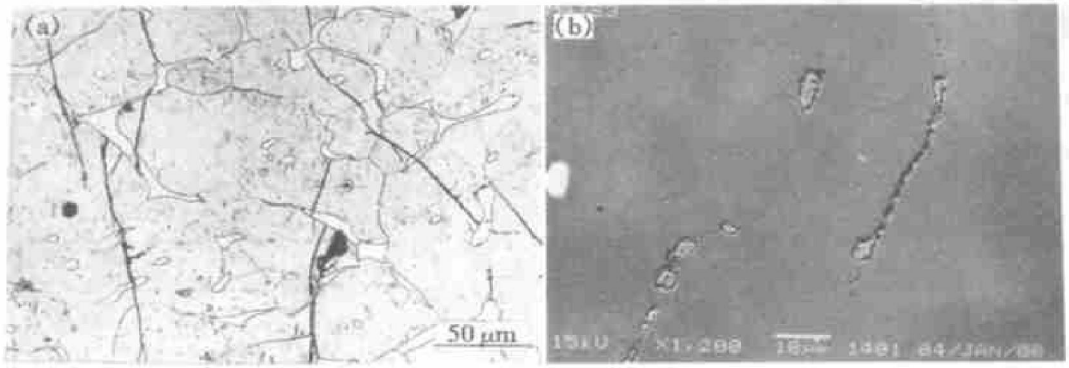

Fig. 5 Microstructure of Mo_4TiSi_3 alloy
(a) —Optical micrograph; (b) —Back-scattered electron micrograph

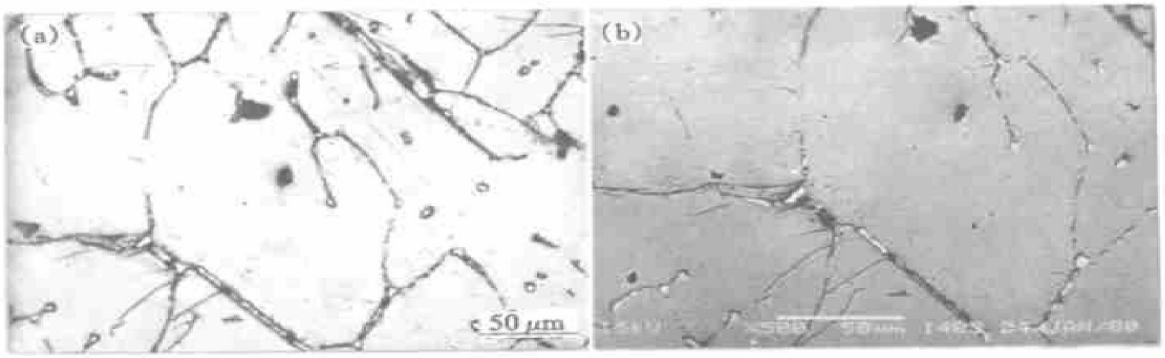

Fig. 6 Microstructure of Mo_4VSi_3 alloy
(a) —Optical micrograph; (b) —Back-scattered electron micrograph

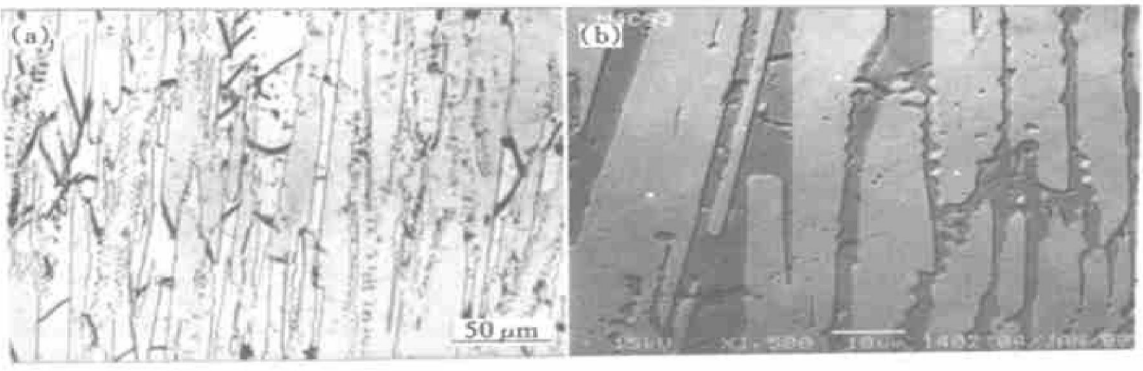

Fig. 7 Microstructure of Mo_4CoSi_3 alloy
(a) —Optical micrograph; (b) —Back-scattered electron micrograph

Table 4 Solubility of transition metal elements in Mo_5Si_3 (mole fraction, %)

Solute element	Zr	Ti	Co	V
Solubility	2.20 ± 1.42	15.94 ± 0.18	3.33 ± 0.76	7.43 ± 0.22

solubility in homogenized Mo_5Si_3.

It is pointed out in the theory of alloying that the atomic size, the electronegativity, the electron configuration and the crystal structure of constituent elements are important factors affecting the formation and stability of alloy phases as well as the solubility of elements. The atomic radius of alloying elements that are supposed to substitute Mo in Mo_5Si_3 are tabulated in Table 5. If the atomic size factor is taken into account, Ti, V have larger solubility because of their small atomic size difference relative to Mo.

Table 5 Atomic radius of substitutions for Mo in Mo_5Si_3 structure

Element	Zr	Ti	Co	V
Atomic radius/ Å	1.60	1.47	1.25	1.34
$r(Me)/r(Mo)$	1.1511	1.0576	0.8993	0.9640

$r(Me)$ —Atomic radius of alloying element

3.4 Microhardness of alloy

The microhardness of the alloys is listed in Table 6. The microhardness of the second phase in alloy 2# and 4# is higher than that of the matrix. On the contrary, the hardness of the matrix is higher in alloy 1# . In alloy 3# and 5# , the second phase particles are so small that their hardness can't be measured. The microhardness of Mo_5Si_3 phase is 11 ~ 13 GPa, which is consistent with data obtained by other authors[6].

Table 6 Microhardness of alloys

Alloy number	Hardness of matrix / GPa	Hardness of second phase / GPa
1#	13.47	11.97
2#	11.83	14.49
3#	11.42	–
4#	13.26	14.66
5#	13.46	–

4 CONCLUSIONS

1) The transition metal elements Zr and Co have limited solubility in homogenized Mo_5Si_3 which are determined to be 2.20 ± 1.42, 3.33 ± 0.76 (mole fraction, %) respectively. Under the same condition, transition elements Ti and V exhibit larger solubility, which are determined to be 15.94 ± 0.18, 7.43 ± 0.22 (mole fraction, %), respectively.

2) All studied alloys have a two-phase microstructure. Besides the Mo_5Si_3 matrix, a second phase is present in those alloys, such as $Mo_{37}Zr_{20}Si_{43}$, $Mo_{66}Ti_{15}Si_{19}$, MoCoSi or $(Mo, V)_3Si$.

3) The morphologies and volume fraction of the second phase in homogenized Mo_5Si_3 base alloys are dependent on the alloying elements and different from each other.

[REFERENCES]

[1] YI Dan-qing, LAI Zong-he, LI Chang-hai, et al. Microstructure and fracture behavior of $MoSi_2$ and $MoSi_2$-SiC composite [A]. Proc of the 4th European Conference on Advanced Materials and Processes [C]. Padua/ Venice, 1995, 1: 445– 448.

[2] WANG De-zhi, LIU Xin-yu, ZUO Tie-yong, et al. Effect of ball milling condition on formation of $MoSi_2$ [J]. The Chinese Journal of Nonferrous Metals, 1998, 8(4): 600– 604.

[3] MA Qin, YAN Bing-jun, KANG Mo-kuang, et al. Development and applications of metal silicides [J]. Rare Metal Materials and Engineering, (in Chinese), 1999, 8 (1): 10– 13.

[4] Celis P B, Ishizaki K. Synthesis of intermetallics for high temperature structural applications [J]. J Materials Science, 1991, 26: 3497– 3502.

[5] Kumor K S. Intermetallic Compounds: Vol. 2 [M]. Westbrook J H, Fleischer R L ed. John Wiley & Sons Ltd, 1994. 211.

[6] YI Dan-qing, DU Ruo-xin, CAO Yu. Physical metallurgy of M_5Si_3-type silicides [J]. Acta Metallurgica Sinica, (in Chinese), (accepted).

[7] YI Dan-qing. Structural Silicides—Processing, Microstructure and Toughening [D]. Chalmers University of Technology, Sweden, 1997.

[8] Aoki A, Izumi O. Improvement in room temperature ductility of the L12 type intermetallic compound Ni_3Al by boron addition [J]. Nippon Kinzoku Gakkaishi, 1979, 43: 1190– 1196.

[9] Yi D Q, Li C H. Ternary alloying study of $MoSi_2$ [J]. Metall Mater Trans, 1998, 29A: 119– 126.

[10] Lai Z H, Yi D Q, Li C H. Precipitation of Mo_9FeSi_6 in $MoSi_2$ [J]. Scripta Metallurgica, 1994, 31(7): 815– 818.

[11] Eason P D, Ross E A, Dempere L D, et al. Processing, microstructure and mechanical properties of Mo silicides and their composites [J]. Trans Nonferrous Met Soc China, 1999, 9(Suppl. 1): 1– 12.

(Edited by YANG Bing)